Variations of atmospheric PAHs concentrations, sources, health risk, and direct medical costs of lung cancer around the Bohai Sea under the background of pollution prevention and control in China

Wenwen Ma[1,4,5], Rong Sun[1,4,*], Xiaoping Wang[3], Zheng Zong[1,4], Shizhen Zhao[2], Zeyu Sun[1,4,5], Chongguo Tian[1,4,*], Jianhui Tang[1,4], Song Cui[6], Jun Li[2], Gan Zhang[2]

[1] CAS Key Laboratory of Coastal Environmental Processes and Ecological Remediation, Yantai Institute of Coastal Zone Research, Chinese Academy of Sciences, Yantai Shandong 264003, P.R. China

[2] State Key Laboratory of Organic Geochemistry, Guangzhou Institute of Geochemistry, Chinese Academy of Sciences, Guangzhou, 510640, China

[3] Ludong University, Yantai, 264025, China

[4] Shandong Key Laboratory of Coastal Environmental Processes, Yantai Shandong 264003, P.R. China

[5] University of Chinese Academy of Sciences, Beijing, 100049, China

[6] International Joint Research Center for Persistent Toxic Substances (IJRC-PTS), School of Water Conservancy and Civil Engineering, Northeast Agricultural University, Harbin 150030, China

* Correspondence to: Rong Sun (rsun@yic.ac.cn) and Chongguo Tian (cgtian@yic.ac.cn)

Abstract. The Bohai Sea (BS) as the most polluted area of polycyclic aromatic hydrocarbons (PAHs) in China has been received wide attention in recent decades. To characterize the variations of concentrations and sources of PAHs from June 2014 to May 2019, fifteen congeners of PAHs ($\sum_{15}$PAHs) were measured from atmospheric samples (N=228) collected at 12 sites around the BS, and health risk and direct medical costs associated with lung cancer exposed to PAHs were also estimated. The annual daily average concentration of $\sum_{15}$PAHs was 56.78 ± 4.75 ng m^{-3}, dominated by low molecular weight (LMW-PAHs, 3-ring) (58.7 ± 7.8%). During the five-year sampling period, the atmospheric $\sum_{15}$PAHs concentration reduced by 17.5% for the whole BS, especially in the tightly controlled area of Tianjin (TJ) with a drop of 51.7%, which was mainly due to the decrease of high molecular weight PAHs (HMW-PAHs, 5-6 ring) concentration. Generally, the concentration of $\sum_{15}$PAHs was the highest in winter and the lowest in summer, mainly attributed to the change of LMW-PAHs concentration. Based on PMF model, PAHs at the BS were mainly ascribed to coal combustion and biomass burning. And the contribution of coal combustion and motor vehicle to PAHs had a different performance between the BS (coal combustion rose by ~~6.7~~7.2%, motor vehicle fell by ~~22.7~~22.4%) and TJ (coal combustion fell by ~~13.2~~12.6%, motor vehicle rose by ~~6.7~~6.9%). The incidence of lung cancer (ILCR) caused by exposing to atmospheric PAHs at the BS and TJ decreased by 74.1% and 91.6% from 2014 to 2018, respectively. That was mainly due to the decrease of the concentration of highly toxic HMW-PAHs. It was reflected on the savings of $10.7 million in direct medical costs of lung cancer exposed PAHs, which was accounted 46.1% before air prevention and control around the BS. And there was a higher cost reduction of 54.5% in TJ. Hence, this study proved that implementing pollution prevention and control not only effectively reduced the concentration of pollutants and the caused risks, but also significantly reduced the medical costs of diseases caused by corresponding expose.

1 Introduction

Polycyclic aromatic hydrocarbons (PAHs) were a class of classical organic compounds with at least two benzene rings, and have been received long-term attention because of cytotoxic, teratogenic, mutagenic, or carcinogenic (Colvin et al., 2020; Marvin et al., 2020). The United States Environmental Protection Agency (USEPA) identified sixteen PAH congeners as priority pollutants (Lv et al., 2020). Previous studies were shown that PAHs in the atmosphere of heavily polluted areas such as factories and the urban posed a threat to human health, especially the respiratory system (Agudelo-Castañeda et al., 2017; Ramírez et al., 2011). Because of their relatively high concentration, strong toxic potency, and long-term distance transmission, ~~The~~ the ~~sixteen~~ PAHs congeners in the atmosphere were considered as a major ~~portion~~ factor of lung cancer risk to the public ~~because of their relatively high concentration, strong toxic potency, and long-term distance transmission~~ (Ma et al., 2010; Gong et al., 2011; Ma et al., 2013; Hong et al., 2016). According to the statistics, the incidence and mortality of lung cancer were ranked first among cancer-related cases in the world, and so the lung cancer risk owing to exposing to PAHs was of particular concern and widely assessed (Křůmal and Mikuška, 2020; Liao et al., 2011; Taghvaee et al., 2018; Zhang et al., 2023)~~(Jia et al., 2011; Zhuo et al., 2017; Lian et al., 2021)~~.

PAHs were emitted primarily via incomplete combustion and pyrolysis of carbon-contained materials, such as fossil fuels and biomass (Biache et al., 2014). China has been assessed as the largest emitter of PAHs all over the world for recent two decade because of rapid development of the economy and increasing consumption of carbon-contained materials (Zhang et al., 2007~~).~~), particularly at the Bohai economic zone, as the third developing economic pole. (Sun et al., 2022). PAHs pollution in the atmosphere of the Bohai Sea (BS) was in a severe situation (Wang et al., 2018). The Bohai economic zone included the Beijing-Tianjin-Hebei (BTH) region, the Liaodong Peninsula, and the Shandong Peninsula. The BTH region was the center of economic development of the Bohai Rim economic area. (Liang et al., 2018; Zhang et al., 2016) Hence, the Beijing-Tianjin-Hebei (BTH) region was one of the regions with the highest PAHs emission intensity and the heaviest atmospheric PAHs concentrations in China (Zhang et al., 2007; Zhang et al., 2016). In such

serious pollution, the health risk exposed to PAHs caused great concern. The population attributable fraction (PAF) for lung cancer caused by inhalation of PAHs in the atmosphere of the BTH area was more than twice higher than the mean value in whole China in 2009 (Zhang et al., 2009). The incremental lifetime cancer risk (ILCR) of the PAHs exposure at Tianjin was in the range of 1×10^{-5} to 1×10^{-3} in 2008, which was much higher than the mean level of 4.56×10^{-6} in China (Lian et al., 2021; Bai et al., 2009). The annual lung cancer morbidity of Tianjin (6.99×10^{-6}) within the BTH region was the highest city among 35 cancer registries in China (Zhang et al., 2007). Meanwhile, with the frequent occurrence of haze in the BTH region, more attention has been paid to concentration levels and health risk of fine particulate matter with aerodynamic equivalent diameter ≤ 2.5 μm ($PM_{2.5}$) since 2013 (Chen et al., 2020).

$PM_{2.5}$ pollution in China has obviously been improved since the Air Pollution Prevention and Control Action Plan (2013-2017) and the Three-year Action Plan for Winning the Blue-Sky Defense Battle (2018-2020) were proposed by the Chinese government in 2013 and 2018 (Zhao et al., 2023). As one of the ~~most~~ severely polluted area in China, the improvement was more significantly at the BTH region, which implemented the strictest pollution control policy (Li et al., 2020). As reported that the concentration of $PM_{2.5}$ at the BTH region dropped by 52% from 106 μg m^{-3} in 2013 to 51 μg m^{-3} in 2020 (Bulletin of the State of China's ecological Environment, 2021). In the prevention and control of pollution policies, reducing emissions of coal combustion and motor vehicle were the major parts (Guo et al., 2018; Li et al., 2019). The two sources have been recognized as primary contributors to PAHs in the atmosphere as well (Lin et al., 2015; Han et al., 2018). As a result, the controls of the two sources not only reduced $PM_{2.5}$ emission, but also PAHs emission (Zhi et al., 2017). During the controlling processes, the variations in the concentrations and health risk of $PM_{2.5}$ at BTH region have been well identified (Fang et al., 2016; Yan et al., 2019), while the relevant understanding of PAHs in the region urgently needs to be updated. Especially, the statistical data of the lung cancer risk due to exposing to PAHs was established ten years ago (Zhang et al., 2009; ~~Bai~~ Lian et al., ~~2009~~2021).

To track changes in concentrations and source of atmospheric PAHs and estimate health risk and the direct medical costs associated with lung cancer by exposing to PAHs during the air pollution control actions, a field monitoring campaign was conducted at twelve sites around the BS for five years from June 2014 to May 2019. ~~The BS is the only inland sea in China, and surrounded by the BTH region, the Liaodong Peninsula, and the Shandong Peninsula (Liu et al., 2020).~~ The measures for air pollution control implemented were different at the BTH region, the Liaodong Peninsula, and the Shandong Peninsula (Huang et al., 2017). Thus, it would provide us an opportunity to understand the difference in environmental concentrations, source contributions, and health risk of PAHs. The main aims of this study were (1) to characterize the spatial and temporal changes of the concentrations and components of PAHs in the atmosphere around the BS, (2) to evaluate the difference of source contributions of PAHs, and (3) to assess the changes of direct medical costs for treating lung cancer caused by inhalation exposure to PAHs under atmospheric prevention and control in the five years.

2 Materials and methods

2.1 Sampling site and sample collection

The sampling sites for this study had been reported in previous literatures (Sun et al., 2021), and it was briefly introduced here. The information of the sites was shown in Table S1 of the Supporting Information (SI). Twelve air sampling sites were located at Beihuangcheng (BH), Dalian (DL), Donggang (DG), Dongying (DY), Gaizhou (GZ), Longkou (LK), Laoting (LT), Rongcheng (RC), Tianjin (TJ), Xingcheng (XC), Yantai (YT), and Zhuanghe (ZH). A passive air sampler with polyurethane foam (PUF, 14.00 cm diameter × 1.35 cm thickness) was used to collect atmospheric samples at each sampling site (Eng et al., 2014). The PUF disks were deployed around 1.5–2.0 m above the ground, the sampling duration was about 3 months for one batch. 228 samples were collected from June 2014 to May 2019. The sampling rate of atmospheric PAHs was 3.5 m^3 day^{-1} (Jaward et al., 2005; Moeckel et al., 2009). Prior to sampling, the PUF disks were pre-cleaned by

methanol, acetone, and hexane, respectively. The extracted PUF disks were placed in airtight containers and stored at −18 °C before the sampling campaign. After sampling, the samples were prepared and then stored at a −18 °C freezer in the lab for further analyses.

2.2 Sample pretreatment and instrumental analysis

The five PAHs surrogates (Naphthalene-D_8, Acenaphthene-D_{10}, Phenanthrene-D_{10}, Chrysene-D_{12}, Perylene-D_{12}) and the activated copper fragments were added in advance (Qu et al., 2022). The samples were extracted for 24 h, which the elution was acetone and hexane (200mL, v:v=1:1) through Soxhlet apparatus. The extracted solution was concentrated to 1mL with rotary evaporator (SHB-III, Zhengzhou Greatwall Ltd., China). Then, silica-alumina column was used to obtain the aromatic components, then the targets were obtained with 40 mL of a mixed solution of dichloromethane and hexane (v:v=1:1). Finally, the eluent was concentrated and reduced to 500 μL by a gentle nitrogen stream. As the internal standard substance, 400 ng of hexamethylbenzene (Supelco, USA) was added to each sample solution before the instrumental analysis.

The targets were detected through the gas chromatograph equipped with mass spectrometry (GC-MS, Agilent 5975C-7890A, USA), and the chromatographic column was DB-5MS (Agilent Technologies, 30 m × 0.25 mm × 0.25 μm). Each extract was injected by 1 μL with splitless mode. High-purity helium (purity ≥ 99.99%) with a flow rate of 1.3 mL min^{-1} was used as the carrier gas. The process of oven temperature was set as at 80 ºC with a hold of 3 minutes, and then raised to 310 ºC by 10 ºC min^{-1}, and then hold 10 minutes. The temperatures of inlet and ion source were 290 ºC and 230 ºC, respectively. The details of the targeted compounds were shown in Table S2 of SI. Seven gradients of mixed solutions were established for quantitative calculation of PAHs. More details were reported in previous study (Wang et al., 2018).

2.3 Quality assurance and quality control

The mean recovery values of Naphthalene-D_8, Acenaphthene-D_{10}, Phenanthrene-D_{10}, Chrysene-D_{12}, and Perylene-D_{12} were 77.3%, 85.9%, 87.5%, 88.3%, and 92.8%, respectively, which were ranging from 66.5% to 123.1%. All the relative deviations were within 20%, except for Naphthalene-D_8. Nap was excluded because of its low recovery, and the other fifteen PAHs (Σ_{15}PAHs) were

used for further discussion in this study. For each batch of twelve PUF samples, a field blank and a procedural blank were also analyzed at same treatment process. In this study, the method detection Limits (MDLs, defined as the mean blank value plus 3 times the standard deviation) for 15 PAH congeners ranged from 0.~~016~~ 02 to 0.~~126~~ 13 ng sample^{-1}, which were shown in Table S2 of SI. The final concentrations were not surrogate-corrected. The glassware was all cleaned and burned for 8 hours in muffle oven at 450 ºC before the experiment. The solvents were chromatography-pure or had been redistilled and purified before using.

2.4 Source apportionment of PAHs

The model of positive matrix factorization (PMF) released by the USEPA (PMF 5.0) was used to apportion the emission sources of PAHs in this study. The basic calculation formula of the PMF method is as Eq. (1):

$$x_{ij} = \sum_{k=1}^{p} g_{ik} f_{kj} + e_{ij} \quad (1)$$

where p represents the number of sources identified by the PMF model. x_{ij} represents original concentration data of i^{th} chemical species and j^{th} sample. f_{ik} represents the source profile of k^{th} source and j^{th} chemical species. g_{kj} represents contribution ratio of k^{th} source to j^{th} sample. e_{ij} represents the simulated residual error of i^{th} chemical species and j^{th} sample. Source contributions and profiles are solved by the PMF model minimizing the objective function Q, as Eq. (2):

$$Q_{min} = \sum_{i=1}^{n}\sum_{j=1}^{m}\left(\frac{x_{ij} - \sum_{k=1}^{p} g_{ik} f_{kj}}{u_{ij}}\right)^2 \quad (2)$$

where x_{ij}, g_{ik}, and f_{kj} are same that in Eq. (1), respectively. u_{ij} is the uncertainty of x_{ij}, and the calculation method of uncertainty is showed in Text S2 of SI. More details have been documented (Sofowote et al., 2011; Paatero et al., 2014).

Before the source apportionment, principal component analysis (PCA) was applied to pre-estimate the minimum number of emission sources in this study because PCA was able to explain

the overall variables with fewer variables with a minimum loss of information (Liu et al., 2021). SPSS Statistics 25.0 was used to perform the PCA analysis in this study.

2.5 Health risk assessment

The total toxicity equivalent (*TEQ*, ng m^{-3}) of the fifteen PAHs with *BaP* as reference is calculated as Eq. (3):

$$TEQ = \sum_{i=1}^{n} (C_i \times TEF_i) \quad (3)$$

where C_i is concentration of the i^{th} PAH compound (ng m^{-3}), TEF_i is the cancer potency of the i^{th} PAH compound (dimensionless), as shown in Table S2 of SI.

ILCR in this study referred to cancer risk in a population due to exposure to a specific carcinogen (Zhuo et al., 2017). Its calculation formula is as Eq. (4):

$$ILCR = UR_{BaP} \times TEQ \quad (4)$$

In above, UR_{BaP} represents the cancer risk when the concentration of *BaP* is 1 ng m^{-3} (ng m^{-3}). According to the regulations of World Health Organization (WHO), UR_{BaP} can be 8.7×10^{-5} per ng m^{-3}. That is, in terms of life span of 70 years, lifetime exposure to *BaP* concentration of 1 ng m^{-3} resulted in a risk of cancer by inhalation of 8.7×10^{-5} (Luo et al., 2021).

2.6 Medical costs assessment

In this study, the medical costs were assessed by comparing total direct medical costs for treating lung cancer caused by respiratory exposed to PAHs in the atmosphere under the assumption that no air pollution control and the actual implementation of air pollution control. The total direct medical costs for treating lung cancer (C_t) are calculated as Eq. (5):

$$C_t = C_{pc} \times P \times I_{add} \quad (5)$$

where C_t is the total direct medical costs of lung cancer induced by PAHs exposure, C_{pc} is the per capita direct medical costs of lung cancer, and a cost of $8,700 in China in 2014 was used in this study (Shi et al., 2017). *P* is the annual population, I_{add} is the additional incidence of lung cancer due to PAHs inhalation exposure, it is calculated as Eq. (6):

$$I_{add} = I \times PAF \quad (6)$$

where I is the incidence of lung cancer. And the I value was 87.37×10^{-5} at Tianjin estimated in 2012, which was referred in this study (Cao et al., 2016). *PAF* is the population attributable fraction, defined as the decrease in the incidence or mortality of a disease when a certain risk factor is completely removed or reduced to another lower reference level (Menzler et al., 2008). The *PAF* can be calculated as Eq. (7):

$$PAF = \frac{rr(TEQ)-1}{rr(TEQ)} \text{ and } rr(TEQ) = [URR_{cum,\exp=100}]^{(TEQ\times70/100)} \quad (7)$$

where *rr* is relative risk, that is, the risk of exposure to a specific concentration relative to no exposure. *URR* is the unit relative risk, a reference value of 4.49 per 100 μg m^{-3} years of *BaP* exposure was adopted in this study (Zhang et al., 2009). This reference value was based on an epidemiological study on lung cancer conducted in Xuanwei, China (Menzler et al., 2008) (Gibbs et al., 1997). This study assumed that the mean life expectancy in China was 70 years, and the lifetime exposure was equivalent to 70 years.

3 Results and discussions

3.1 Concentration and composition of PAHs

3.1.1 General information of PAHs

Figure 1 summarizes the annual daily average concentrations of 15 PAHs in the atmosphere at the twelve sampling sites around the BS from June 2014 to May 2019. The annual daily average concentration of Σ_{15} PAHs around the BS was 56.78 ± 4.75 ng m^{-3}, with a range of 51.~~4~~39 – 63.~~6~~55 ng m^{-3}. And the highest concentration was the low molecular weight PAHs (LMW-PAHs, 3-ring), followed by middle molecular weight PAHs (MMW-PAHs, 4-ring) and high molecular weight PAHs (HMW-PAHs, 5-ring and 6-ring), which were accounting for 58.7%, 34.8%, and 6.~~65~~7% of the total concentration, respectively. The atmospheric PAHs concentration was dominated by the LMW-PAHs in this study, which Phe, Fla, and Flu were the main compounds accounting for 37.7%, 19.8%, and 12.6% of the total. The atmospheric PAHs concentrations around the BS were at a higher pollution level than the Yangtze River Delta and the Pearl River Delta, such as

Ningbo (45 ng m^{-3}) (Tong et al., 2019) and Guangzhou (9.72 ng m^{-3}) (Yu et al., 2016). And the atmospheric concentrations of PAHs around the BS were also much higher than in atmosphere above the Great Lakes (1.3 ng m^{-3}) (Li et al., 2021) and southern Europe cities (3.1 ng m^{-3}) (Alves et al., 2017). Overall, it was found that the pollution of atmospheric PAHs around the BS was still worrying.

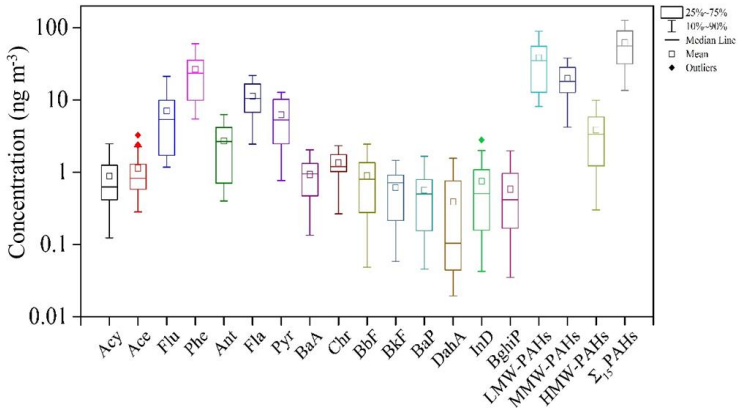

Figure 1. Atmospheric concentrations of polycyclic aromatic hydrocarbons (PAHs) around the BS from June 2014 to May 2019.

3.1.2 Temporal variations of PAHs

For seeking better understand the variation characteristics of PAHs in the atmosphere, the summer of the previous year to the spring of the next year were taken as a statistical cycle. The concentrations of Σ_{15}PAHs in the five annual cycles around the BS were 63.~~6~~55 ± 58.43 ng m^{-3} (2014-2015), 55.50 ± 37.94 ng m^{-3} (2015-2016), 60.90 ± 31.13 ng m^{-3}, (2016-2017), 51.439 ± 29.41 ng m^{-3} (2017-2018), and 52.50 ± 40.~~1~~08 ng m^{-3} (2018-2019), respectively (Table S3 of SI). Overall, the concentrations of Σ_{15}PAHs from June 2014 to May 2019 showed a slow downward trend with a decrease of 17.5%. The decrease of atmospheric PAHs concentrations was mainly due to the

decline of the HMW-PAHs concentrations. The HMW-PAHs composition ratio decreased from 11.3% (2014-2015) to 3.44% (2018-2019), while the MMW-PAHs raised from 35.5% (2014-2015) to 41.2% (2018-2019). The LMW-PAHs composition ratio was stable from 53.4% (2014-2015) to 55.4% (2018-2019). The one factor that effected the concentrations of PAHs in the atmosphere after they were discharged from the emission source was meteorological conditions (Fan et al., 2021), and the other important factor was the amount of the direct emission from the emission source (Ma et al., 2018). The sources of PAHs with different ring numbers were different (Li et al., 2021). LMW-PAHs were mainly produced in the combustion process of non-petroleum sources, while HMW-PAHs were mainly from high temperature combustion products generated by fossil fuel combustion, including some activities involving pyrolysis process, such as vehicle emissions, industrial productions, and other high-temperature source emissions (Zhang et al., 2018; Xing et al., 2020). The significant decrease of HMW-PAHs concentrations at the BS during the five-year observation period might be related to the decrease of high temperature emission sources. Due to the high toxicity characteristics of HMW-PAHs (Biache et al., 2014; Ma et al., 2020), the decrease of its concentration might indicate a decrease in the environmental toxicity of PAHs.

The seasonal distributions of PAHs concentrations in the atmosphere of the BS region showed high in cold season and low in warm season. The concentrations of Σ_{15}PAHs in four seasons were as follow: winter (104.32 ± 9.50 ng m^{-3}) > autumn (53.94 ± 9.10 ng m^{-3}) > spring (43.89 ± 19.54 ng m^{-3}) > summer (26.~~3~~28 ± 13.42 ng m^{-3}) (Table S5 of SI). The concentration of PAHs in winter was about 4 times higher than that in summer, and the maximum and minimum of the annual daily average concentrations at 12 sampling point mostly occurred in winter and summer. In addition, there were significant differences between total PAHs concentration and different ring number concentrations ($p < 0.05$, the difference level is shown in Table S6 of SI). The seasonal characteristics of PAHs concentrations in this study were consistent with reported results in North China (Ma et al., 2017; Zhang et al., 2019). Interestingly, it was that the difference of PAHs concentrations in four seasons was mainly on account of LMW-PAHs. ~~This indicated that there were other important pollution sources for LMW-PAHs, followed by MMW-PAHs, which was significantly increasing~~

~~in winter at the BS region.~~ This indicated that there were nonnegligible pollution sources for LMW-PAHs, especially in winter at the BS region. Then identifying the source of LMW-PAHs was crucial for improving environmental quality of the BS. Studies have shown that coal burning emissions and biomass burning were the main sources of atmospheric PAHs in this region (Liu et al., 2019). In terms of the per capita fuel consumption spatial distribution, the north and west China were apparently higher than that of southeast China, principally because of the difference in winter heating fuel consumption. Therefore, there were significant seasonal variations of per capita fuel consumption, with peak consumption in the winter months being about twice as high as in the summer months. (Zhu et al., 2013)~~For typical northern families, the consumption of firewood burning and coal in winter was 1.5–2.0 times higher than that in summer due to heating and other activities (Qin et al., 2007). As a result, PAHs emissions in winter were at least 1.5 times higher than those in summer~~. In addition, due to the migration characteristics of atmospheric PAHs, meteorological conditions such as temperature and wind direction in different seasons would also affect the observed concentration (Tan et al., 2006). And low temperature and inversion layer in winter were not conducive to atmospheric diffusion, resulting in a relatively high concentration of PAHs in the atmosphere near the surface (Wang et al., 2018).

3.1.3 Spatial characteristics of PAHs

Figure 2 and Table S7 of SI displays the distribution of the five-year mean concentrations of Σ_{15} PAHs from June 2014 to May 2019 at the 12 sampling sites around the BS. The concentrations of atmospheric Σ_{15}PAHs ranged from 25.92 ± 6.41 ng m^{-3} (RC) to 103.71 ± 39.11 ng m^{-3} (XC). The concentrations of PAHs on the BS north coast were twice higher than at the BS south coast. PAHs were a class of pollutants that can undergo long-range transport in the atmosphere (Wang et al., 2018), and their spread was largely affected by local meteorological conditions (Ding et al., 2005). The climate in North China and the adjacent oceanic area was greatly affected by the East Asian monsoon, and the characteristic weather phenomenon in the winter monsoon was the strong north and northwest winds (Tian et al., 2009). Due to the additional emissions from fuel consumption for domestic heating in the source areas, the atmospheric PAHs concentrations significantly increased

(Feng et al., 2007; Gao et al., 2016). Combined with backward trajectory shown in Fig. S4 of SI, it suggested that the elevated PAH concentrations in winter at the north of the BS were mainly attributed to their outflow from the north and northwest source regions carried by the winter monsoon winds. According to the distribution of atmospheric PAHs in some representative parts of northern China, it was found that the Beijing-Tianjin-Hebei region was greatly affected by nearby sources, while Shandong province and other places were mainly affected by regional emissions. (Zhang et al., 2016) However, the composition of PAHs at the north-south showed consistency without no significant differences (Table S8 of SI). As the whole, the composition of PAHs at 12 station that the highest content was LMW-PAHs (North: 60.0%, South: 57.4%), followed by MMW-PAHs (North: 32.7%, South: 32.4%), and HMW-PAHs was the lowest (North: 7.3%, South: 10.8%). The above indicated that there were the same emission sources of PAHs in the atmosphere around the BS.

However, for TJ, the study found that there was a more significant change in the concentration of atmospheric PAHs, which decreased from 68.61 ng m^{-3} (2014-2015) to 33.14 ng m^{-3} (2018-2019). The reason was mainly that TJ was located at the Beijing-Tianjin-Hebei region where was the strictest area of air pollution prevention and control, as a key area in China's "12th Five Year Plan". For exploring the potential differences of source emissions at 12 sampling points, Pearson correlation analysis was used to analyze the seasonal distribution of PAHs concentrations as shown in Table S9 of SI. Among the five stations (LK, DY, TJ, LT, and XC) at the western BS centered on TJ, the correlation coefficients of atmospheric PAHs concentration (0.72–0.89) among the other four stations were greater than that between each site and TJ (0.50–0.68). That the co-variability of PAHs concentrations between TJ and the other four stations was weaker. This indicated that there were certain differences between TJ's PAHs emission sources and adjacent areas.

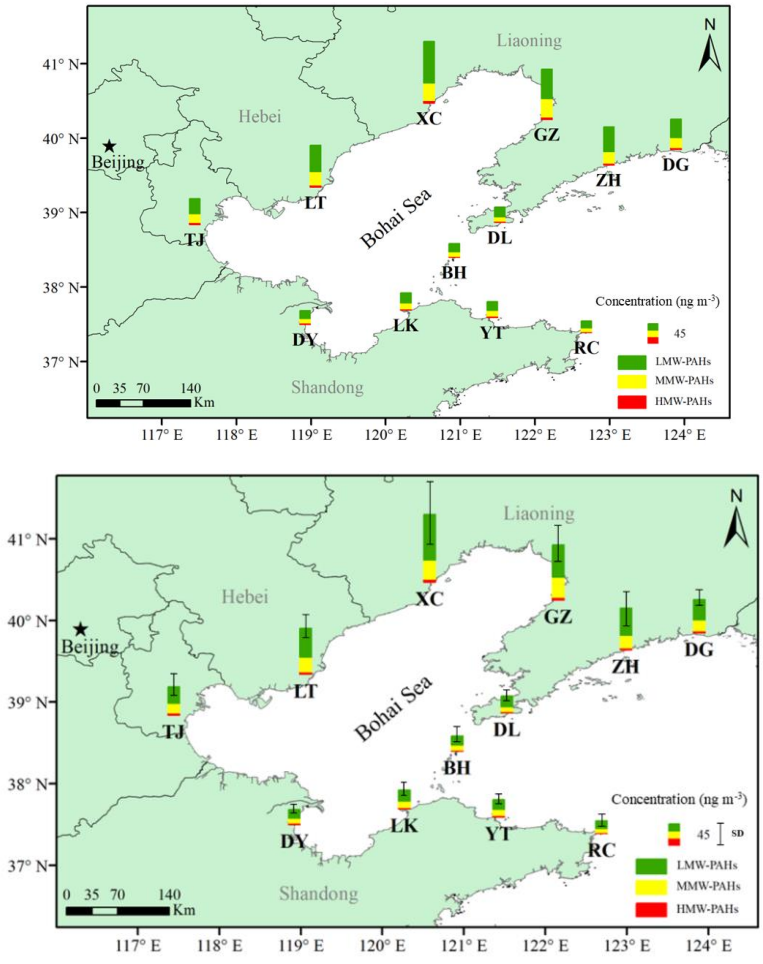

Figure 2. The mean concentration distribution of Σ_{15} PAHs at 12 sites around the BS from June 2014 to May 2019.

3.2 Source apportionment of PAHs

For further probing into the causes for the variations of the concentrations and compositions of PAHs, the sources apportionment of PAHs in the atmosphere around the BS and TJ region from 2014-2015 to 2018-2019 was investigated via PCA and PMF. PCA analysis results showed that when four factors (eigenvalues > 1) were extracted from the data set, the total cumulative load accounted for more than 85% of the variance (Table S10 of SI). This indicated that at least four types of emission sources could better explain the source of atmospheric PAHs. For PMF model, the key process was to determine the correct number of factors, and this study was based on the results of PCA. Based on the random seed, 4 – 7 factors were used through the PMF model for source analytical simulation. The source analytical simulation of five factors determined the most stable results and the most easily interpreted factors. The solution produces Q values (both robust and true) that were close to the theoretical Q values, which was indicating that the PAHs data set in the modeling input provided appropriate uncertainty (Sun et al., 2021). The data set used for PMF analysis included the concentrations of 228 samples of 15 PAHs and uncertainties. The diagnostic regression R^2 value for the overall concentrations of 15 PAHs components was 0.986. The predicted concentrations of 15 PAHs via PMF model were almost consistent with the actual concentrations of 15 PAHs around the BS (Fig. S5–S6 of SI and Text S2 of SI). It meant that the model results were good and could be used as the judgment basis for source analysis of target species, so these 5 factors would well explain the source of PAHs. Contribution of source identified by PCA and PMF were coal combustion, biomass burning, industrial processes, gasoline emission, and diesel emission. The detailed information of source identification is shown Text S3 of SI.

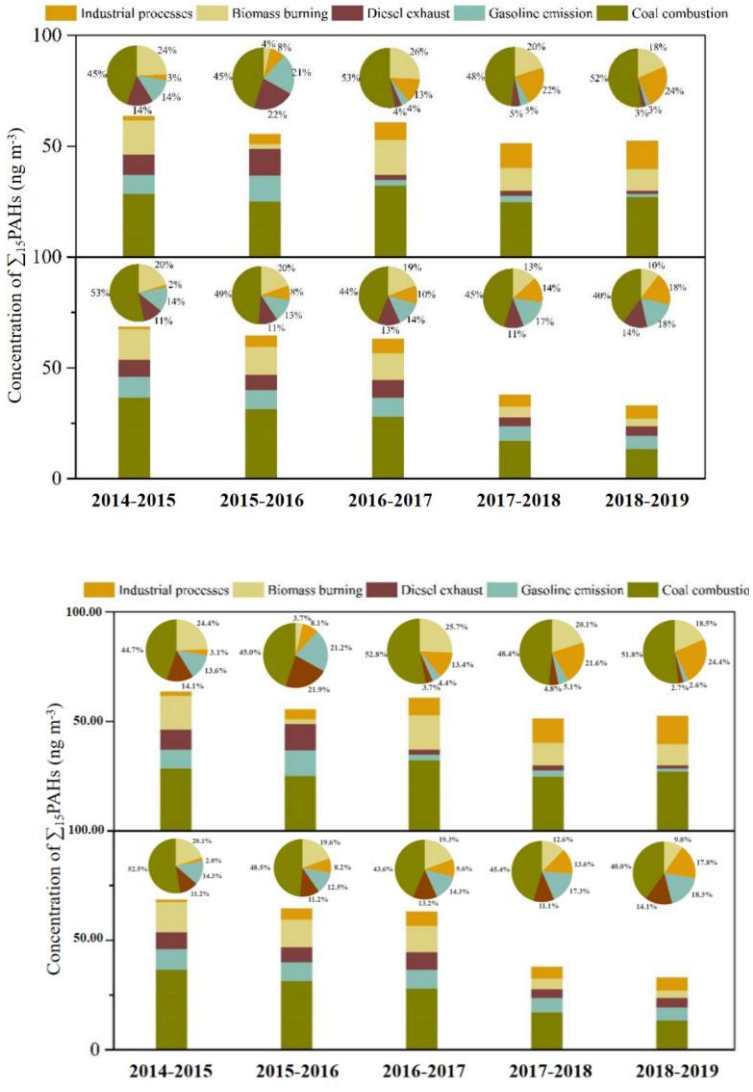

带格式的: 居中

Figure 3. Concentration and source contribution of Σ_{15} PAHs sources around the BS (the upper part) and TJ (the lower part) from 2014-2015 to 2018-2019.

Fossil fuels~~Fuel~~ combustion emissions were the reason for the significant increase of atmospheric pollutants, and that were also responsible for the elevated $PM_{2.5}$ levels around the BS region (Yang et al., 2017). To explore the relationship between Σ_{15}PAHs and $PM_{2.5}$ concentrations, available online $PM_{2.5}$ data for eight cities that on behalf of sampling sites (DG, DL, DY, GZ, LT, TJ, XC, and YT) (Air quality historical data query, 2014-2019) were collected, which averaged their concentrations according to the sampling periods in the study (Table S12 of SI). The Pearson correlation coefficients of the concentrations of atmospheric PAHs and $PM_{2.5}$ were ranging from 0.485 to 0.868, and the significant levels were greater than 95% as listed in Table S13 of SI. During the observation of the five-year, the $PM_{2.5}$ concentration at the BS region decreased by 29.6% from 57 μg m^{-3} to 40 μg m^{-3}, and at TJ showed an even greater decrease by 33.8% from 78 μg m^{-3} to 51 μg m^{-3}. From 2013, $PM_{2.5}$ had been strictly controlled by the government year by year, which the significant correlation indicated that the PAHs concentrations should be affected. To explore the potential influencing factors of the difference in atmospheric PAHs composition between the BS area and TJ, their average annual contributions of various PAHs emission sources from 2014-2015 to 2018-2019 were compared shown in Figure 3. During the sampling period of the BS region, coal combustion was the main source of the atmospheric PAHs emission (~~45~~44.7%), followed by biomass burning (24.4%) in 2014-2015, which was switching to coal combustion (~~52~~51.8%) and industrial processes (24.4%) in 2018-2019. For TJ, coal combustion was also the main source of the atmospheric PAHs emissions (~~53~~52.5%), followed by biomass burning (20.1%) in 2014-2015, which was switching to coal combustion (40.0%), industrial processes (~~18~~17.8%) and gasoline emissions (18.3%) in 2018-2019. The source contributions of coal combustion to atmospheric PAHs had increased by 7.2% around the BS, while the corresponding contributions in TJ had fallen by ~~13~~12.6%. The absolute contribution (the total concentration of PAHs multiplied by the percentage value of the contributing source) decreased, which was indicating that the reduction of the coal contribution source had a significant improvement on the atmospheric PAHs pollution.

The main source of atmospheric PAHs around the BS was coal combustion (Liu et al., 2019; Qu et al., 2022), while for TJ, as one of the key areas for air pollution control in China, had taken stricter measures to control emissions of coal combustion (Wu et al., 2015). For instance, the city took the lead in the switching domestic fuel from coal to natural gas and electricity in 2017 to reduce emissions of air pollutants (Zhang et al., 2021). These targeted measures had more forcefully controlled coal-combustion emissions for PAHs in TJ than the other places around the BS region (Guo et al., 2018). Vehicle emission (gasoline and diesel exhaust) to atmospheric PAHs had experienced a sharp drop of ~~23~~22.4% for the BS area, while for TJ risen by ~~7~~6.9%. The same trend for vehicle emission was found in the study of Beijing and Tianjin (Zhang et al., 2016; Chao et al., 2019). The decrease was mainly due to the elimination and scrapping of substandard vehicles carried out by the Chinese government in 2015. Based on the "China Vehicle Environmental Management Annual Report", the car ownership around the BS increased by about 17.5 million, but the emissions of hydrocarbons including PAHs reduced by 95,000 tons from 2014 to 2018 (Fig. S8 of SI). The source apportionment showed that the contribution of vehicle emission to PAHs had a sharp decline since the spring of 2016 (Fig. S9 of SI), with a decreased by 38% (19% for gasoline and 19% for diesel) around the BS (Huang et al., 2017). Although the contribution of vehicle emissions for TJ was increased, the concentrations of PAHs was decreasing. It indicated that these measures had also controlled vehicle emissions and kept the emissions of PAHs at a low level. Therefore, targeted control measures could effectively control $PM_{2.5}$ and PAHs pollution in the atmosphere at the BS and TJ. Moreover, PAHs were a kind of organic compounds produced with black carbon (BC), and, to some extent, the molecular characteristics of PAHs also provided the basic data to analysis of the source of BC in the atmosphere of the BS (Fang et al., 2016). At the same time, the PAHs source analysis results of this study revealed that the composition and source of atmospheric BC in the BS region have also changed from 2014 to 2019. This problem needs our attention and confirmation.

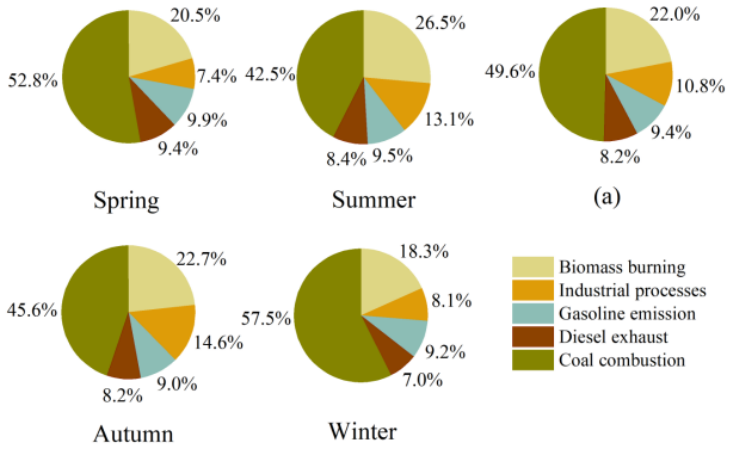

Figure 4. The seasonal and average contributions for five sources of Σ_{15} PAHs derived from PMF; (a): the five-year average contributions of five sources.

Figure 4 shows the seasonal distribution of five sources for atmospheric PAHs at the BS. Generally, the seasonal distribution of five sources for atmospheric PAHs at TJ was consistent with that the BS, which was not separately discussed here. The relevant information of TJ was shown as Fig. S10 of SI. Coal combustion was the main emission source in the four seasons, followed by biomass burning, while the contributions of the others (industrial processes, gasoline emission, and diesel emission) were similar. Compared with other seasons, the contribution of coal combustion for atmospheric PAHs to the BS was the highest in winter, which was followed by spring, and the lowest was in summer. This was consistent with the seasonal distributions of the concentrations of PAHs in the atmosphere at the BS. Based on the seasonal distribution of concentrations, the increase concentrations of atmospheric PAHs in winter were mainly caused by coal combustion. This might be due to people in cold winters at northern China rely on coal combustion for heating. For biomass combustion, it was higher in summer and autumn, which was related to straw burning after harvest. Given all this, the seasonal distributions of PAHs sources indicated that the pollution of atmospheric PAHs was mainly influenced by human activities.

3.3 Health risk exposed to PAHs

On the basis of the Eq. (3), the annual mean *TEQ* value around the BS was 1.37 ± 1.05 ng m^{-3} from June 2014 to May 2019, which below the national standard (10 ng m^{-3}) while slightly higher than the WHO standard (1 ng m^{-3}). The HMW-PAHs contributed dominantly 76.4% of the total *TEQ*. However, the concentration of HMW-PAHs in the atmosphere accounted for 6.5% of the total PAH concentration. Among which, the two major *TEQ* contributors were BaP (38.2% ± 8.0%) and DahA (16.6% ± 9.0%). For TJ, the annual mean *TEQ* value was 1.69 ± 1.50 ng m^{-3}, which was slightly higher than that the BS. It was indicating that higher health risk was caused by PAHs exposed at TJ than around the BS. The HMW-PAHs contributed dominantly 90.9% of the total *TEQ*. However, the concentration of HMW-PAHs in the atmosphere accounted for 8% of total PAHs concentrations. Among which, the two major contributors were BaP (47.2% ± 9.2%) and DahA (19.7% ± 16.2%).

The information of *TEQ* at BS and TJ from June 2014 to May 2019 was shown in Figure 5. The average value of *TEQ* at the BS in the five cycle years was 2.55 ± 1.49 ng m^{-3}, 2.49 ± 1.63 ng m^{-3}, 0.69 ± 0.76 ng m^{-3}, 0.47 ± 0.66 ng m^{-3}, and 0.67 ± 0.84 ng m^{-3}, respectively. The value of *TEQ* at the BS showed a downward trend year by year. The environmental health risk of PAHs in the fifth year was decreased by three times than in the first year. ~~The decrease in the fifth year compared with the first year was more than two times, indicating that the environmental health risk of PAHs was decreasing.~~ It was found that the decrease of HMW-PAHs concentration was the main reason for the decrease of the toxicity of PAHs. For example, the concentration of BaP in the atmosphere at the BS decreased by 79.1% in five years, and the concentration of DahA, as a species with carcinogenic toxicity equivalent to BaP, decreased by 96.1%. For TJ, the average value of *TEQ* in the five cycle years was 3.63 ± 0.14 ng m^{-3}, 3.38 ± 0.72 ng m^{-3}, 0.84 ± 0.38 ng m^{-3}, 0.28 ± 0.10 ng m^{-3}, and 0.31 ± 0.15 ng m^{-3}, respectively. The *TEQ* value of PAHs in the atmosphere decreased by 91.5% at TJ in the past five years. At TJ, BaP and DahA as the major contributing factors of *TEQ* in the atmosphere also showed more significant decline than around the BS. To sum up, the results

showed that pollution control could not only reduce the total concentration of PAHs in the atmosphere at the BS, but also affected the composition of the PAHs. And it mainly affected the concentration of HMW-PAHs compounds, which the total toxic equivalent of PAHs in the atmosphere at the BS was remarkably reduced.

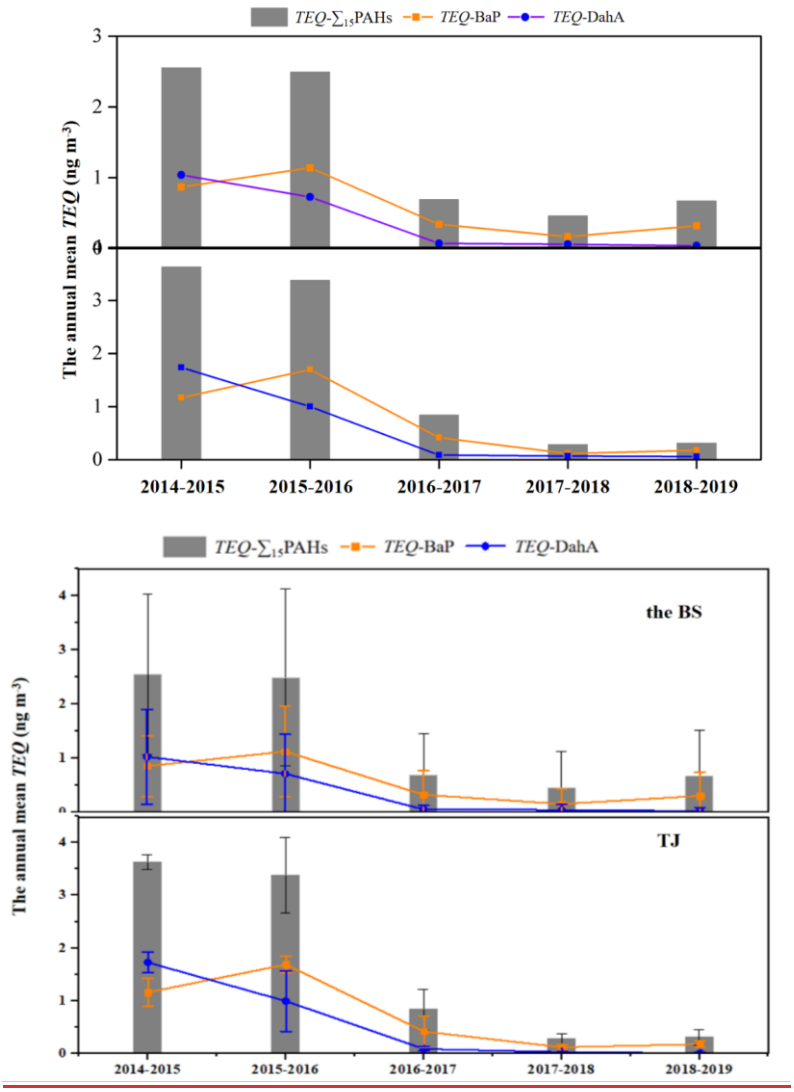

带格式的: 居中, 段落间距段后: 0 磅

446

447 **Figure 5.** The annual mean *TEQ* of 15 PAHs, BaP, and DahA in the atmosphere at the BS (the
448 upper part) and TJ (the lower part) from June 2014 to May 2019.

Simultaneously, incremental lifetime cancer risk (*ILCR*) was used to assess the potential carcinogenic risk of PAHs in the atmosphere at the BS. According to the USEPA, the *ILCR* value less than 1×10^{-6} was an acceptable risk level. When the *ILCR* value was equal to or high than 1×10^{-6} but less than 1×10^{-4}, which was in a serious risk of cancer, and health issues should be taken seriously. When the *ILCR* value were equal to or greater than 1×10^{-4}, it was considered life-threatening for human. The specific calculation was seen Eq. (4). It was found that the range of *ILCR* value of atmospheric PAHs at the BS region for five years was 4.1×10^{-5}–2.2×10^{-4}, with an average value of 1.2×10^{-4}, which means that the risk of cancer in this region was in a serious state, and health problems should be paid more attention to. Similarly, to the above *TEQ*, *ILCR* values were also dominated by HMW-PAHs. The *ILCR* caused by PAHs is listed in Table S14 of SI. The *ILCR* at the BS decreased significantly by 74.1% from 2.2×10^{-4} in the first year to 5.7×10^{-5} in the fifth year. Compared with the BS, the ILCR at TJ decreased more significantly, from 3.2×10^{-4} to 2.7×10^{-5} by 91.6%. As shown in Table S15 of SI, the study found that the concentration variations of highly toxic BaP and DahA were basically synchronized with the changes of *ILCR*, which implied that the decrease of concentrations of both was the main reason for the cancer risk reduction. The significant reduction of cancer risk at the BS region indicated that the emission of highly toxic HMW-PAHs in the atmosphere has been effectively controlled, which also reflected that the prevention and control of air pollution had effectively reduced the health risk. In particular, the reduction effect of PAHs exposure risk was more obvious at TJ, which air pollution control was strict.

3.4. Direct medical costs of lung cancer caused by exposed to PAHs

This reduction of PAHs health risk would lead to a reduction in the number of people who develop cancer, thus saving on the cost of cancer treatment. In this study, the direct medical costs of lung cancer caused by respiratory exposure to PAHs was estimated by the additional incidence of lung cancer caused by PAHs exposure, the population in the study area, and the direct medical costs per capita of lung cancer patients. The specific calculation was seen Eq. (5). In addition to

PAHs exposure, there were many environmental risk factors that could induce lung cancer. For deriving the lung cancer burden caused by atmospheric PAHs respiratory exposure from the incidence of lung cancer, this study was characterized by percentage of population risk attribution (*PAF*). The details were seen Eq. (6) and Eq. (7). *PAF* here represented the percentage of reduction in lung cancer incidence which PAHs, an environmental factor, were completely removed or their concentration was reduced. According to the above introduction of *PAF* and analysis of *TEQ*, the directly calculated *PAF* within five years around the BS ranged from 0.5‰ to 2.7‰, with an average value of 1.4‰. The five-year *PAF* at TJ ranged from 0.3‰ to 3.8‰, with an average value of 1.7‰. A remarkable situation was that *PAF* around the BS region and TJ decreased significantly in the past five years, from 3.8‰ and 2.7‰ in the first year to 0.3‰ and 0.7‰ in the fifth year respectively. The additional lung cancer incidence (I_{add}) due to respiratory exposure to PAHs was calculated using the product of lung cancer incidence and *PAF*. Previous studies reported that the incidence of lung cancer at TJ in 2012 was 87.37×10^{-5} (Cao et al., 2016). In this study, 87.37×10^{-5} was used as the reference value of lung cancer incidence. The average I_{add} caused by respiratory exposure to PAHs around the BS region and TJ were 1.26×10^{-6} and 1.55×10^{-6}, respectively. During the observation of the five-year, the I_{add} around the BS region and TJ decreased from 2.34×10^{-6} and 3.33×10^{-6} in the first year to 6.15×10^{-7} and 2.87×10^{-7} in the fifth year, respectively. The population numbers in the study area were all referred from the public data of the statistical yearbook. The estimated results of the BS region and TJ are shown in Table S16–S17 of SI, respectively. It had been reported that the direct cost of an average case of lung cancer patients in China in 2014 was $9042.79 (Shi et al., 2017; Huang et al., 2016). Since there was no reference data available for other corresponding years, this study took the direct cost per case of lung cancer patients as the baseline in 2014, and the estimate assumed the same direct medical costs per capita for lung cancer within five years.

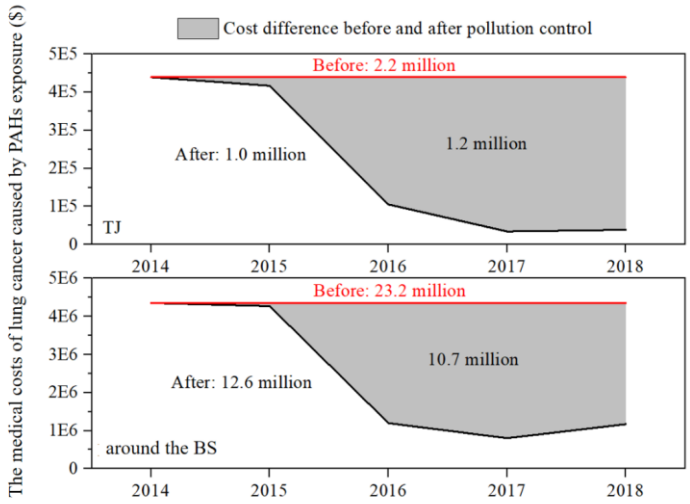

Figure 6. The medical costs of lung cancer caused by PAHs exposure before and after the control of air pollution at TJ and around the BS from 2014 to 2018.

~~Figure 6 shows the comparative results of direct medical costs of lung cancer at the BS region and TJ under two scenarios from 2014 to 2018.~~ Figure 6 shows the comparative results of direct medical costs of lung cancer at the BS region and TJ from 2014 to 2018 under before and after pollution control. In the five years, under the implementation of air pollution control, the total direct medical costs of lung cancer caused by respiratory exposure to PAHs in the Bohai Rim region was $12.6 million. Assuming that no air pollution control was implemented, the total direct medical costs of lung cancer caused by PAHs exposure did not change in five years, and the total direct medical costs was ~~five times in 2014 with an estimated value of~~ $23.2 million. The actual implementation of control on the total direct medical costs of lung cancer saved $10.7 million. At TJ, the total direct medical costs of lung cancer induced by respiratory exposure to PAHs under actual air pollution control was $1.0 million. Under the assumption that no air pollution control was implemented, the total direct medical costs of lung cancer caused by PAHs exposure was $2.2 million,

saving about $1.2 million at TJ. Compared to without air pollution control, the total direct medical costs of lung cancer caused by PAHs exposure decreased by 46.1% around the BS region and by an even greater 54.5% at TJ. This illustrated that the implementation of air pollution control not only reduced the risk of lung cancer caused by PAHs exposure around the BS region, but also created significant health benefit in the direct medical costs of lung cancer, especially in tightly controlled areas such as TJ. Therefore, the above results noted that more precise pollution prevention and control could better reduce the emission of the pollutants, and sequentially reduce the health risk of human expose.

4 Conclusions

A five-year atmospheric PAHs observation was conducted at twelve sites around the BS from June 2014 to May 2019. The five-year atmospheric concentration of Σ_{15}PAHs was 56.78 ± 4.75 ng m^{-3}, characterized by dominant LMW-PAHs (58.7 ± 7.8%). The maximum annual concentrations and seasonal concentrations occurred in the first year and every winter, respectively. The concentrations of $\sum_{15}$ PAHs in the atmosphere reduced significantly around the BS, especially at the sampling site of TJ during the sampling period. The contributions of coal combustion and vehicle emission to PAHs in the atmosphere during the sampling period showed an increase and a decrease around the BS, respectively. However, the variations of coal combustion and vehicle emission in the source contributions in TJ were just the opposite. From 2014 to 2018, the additional lung cancer incidence of lung cancer caused by PAH exposure around the BS dropped by 74.1%, and a higher drop of 91.6% in TJ. From the statistical standpoint, the drop of the incidence saved about $10.7 million for the total direct medical costs of lung cancer caused by PAHs exposure around the BS. Compared to without air pollution control, the total direct medical costs of lung cancer caused by PAHs exposure decreased by 46.1% around the BS region and by an even greater 54.5% at TJ. And it was further be certified that pollution reduction was beneficial to human health. In the fight against air pollution, more precise pollution prevention and control strategies were needed.

Data availability. Corresponding data for the samples can be accessed on request to the corresponding author (Chongguo Tian, cgtian@yic.ac.cn)

Author contributions. CT and ZZ designed the research; WM, RS, XW, ZZ, ZS, and CT conducted the sample collection; WM, RS, and XW performed the chemical analyses; WM, RS, XW, and CT analyzed the data, carried out the simulations and wrote the original article; ZS, SZ, JT, SC, JL, and GZ helped with article submissions. All authors have given approval to the final version of the manuscript.

Competing interests. The contact author has declared that none of the authors has any competing interests.

Acknowledgements. This study was supported by the National Natural Science Foundation of China - Shandong Joint Fund (U1906215) and the National Natural Science Foundation of China (No. 41977190 and 42177089).

Reference

Air quality historical data query: https://www.aqistudy.cn/historydata/, last access: 31 August 2023, 2014-2019.

Alves, C.A., Vicente, A.M., Custodio, D., Cerqueira, M., Nunes, T., Pio, C., Lucarelli, F., Calzolai, G., Nava, S., Diapouli, E., Eleftheriadis, K., Querol, X., and Musa Bandowe, B.A.: Polycyclic aromatic hydrocarbons and their derivatives (nitro-PAHs, oxygenated PAHs, and azaarenes) in $PM_{2.5}$ from Southern European cities, Sci. Total. Environ., 595, 494–504, https://doi.org/10.1016/j.scitotenv.2017.03.256, 2017.

~~Bai, Z.P., Hu, Y.D., Yu, H., Wu, N., and You, Y.: Quantitative health risk assessment of inhalation exposure to polycyclic aromatic hydrocarbons on citizens in Tianjin, China, B. Environ. Contam. Tox., 83, 151–154, https://doi.org/10.1007/s00128-009-9686-8, 2009.~~

570 Biache, C., Mansuy-Huault, L., and Faure, P.: Impact of oxidation and biodegradation on the most
571 commonly used polycyclic aromatic hydrocarbon (PAH) diagnostic ratios: Implications for the
572 source identifications, J. Hazard. Mater., 267, 31–39, https://doi.org/10.1016/j.jhaz-
573 mat.2013.12.036, 2014.
574 Bulletin of the State of China's ecological Environment:
575 http://www.mee.gov.cn/hjzl/sthjzk/zghjzkgb/, last access: 31 August 2023, 2021.
576 Cao, M., Wang, M., and Song, F.: Secular trend of lung cancer incidence in Hexi District, Tianjin,
577 1992 – 2012, Tumor., 36, 1330−1334, https://doi.org/10.3781/j.issn.1000-7431.2016.22.553, 2016.
578 Chao, S.H., Liu, J.W., Chen, Y.J., Cao, H.B., and Zhang, A.C.: Implications of seasonal control of
579 $PM_{2.5}$-bound PAHs: An integrated approach for source apportionment, source region identification
580 and health risk assessment, Environ. Pollut., 247, 685−695, https://doi.org/10.1016/j.en-
581 vpol.2018.12.074, 2019.
582 Chen, C., Fang, J.L., Shi, W.Y., Li, T.T., and Shi, X.M.: Clean air actions and health plans in China,
583 Chinese Medical Journal., 133, 1609−1611, https://doi.org/10.1097/cm9.0000000000000888,
584 2020.
585 Colvin, K.A., Lewis, C., and Galloway, T.S.: Current issues confounding the rapid toxicological
586 assessment of oil spills, Chemosphere., 245, 125585, https://doi.org/10.1016/j.chemo-
587 sphere.2019.125585, 2020.
588 Ding, Y.H., and Chan, J.C.L.: The East Asian summer monsoon: an overview, Meteorol. Atmos.
589 Phys., 89, 117−142, https://doi.org/10.1007/s00703-005-0125-z, 2005.
590 Eng, A., Harner, T., and Pozo, K.: A prototype passive air sampler for measuring dry deposition of
591 polycyclic aromatic hydrocarbons, Environ. Sci. Technol. Let., 1, 77−81,
592 https://doi.org/10.1021/ez400044z, 2014.
593 Fan, L.P., Fu, S., Wang, X., Fu, Q.Y., Jia, H.H., Xu, H., Qin, G.M., Hu, X., and Cheng, J.P.: Spati-
594 otemporal variations of ambient air pollutants and meteorological influences over typical urban
595 agglomerations in China during the COVID-19 lockdown, J. ENVIRON. SCI., 106, 26−38,
596 https://doi.org/10.1016/j.jes.2021.01.006, 2021.

Fang, D., Wang, Q., Li, H., Yu, Y., Lu, Y., and Qian, X.: Mortality effects assessment of ambient $PM_{2.5}$ pollution in the 74 leading cities of China, Sci. Total. Environ., 569-570, 1545–1552, https://doi.org/10.1016/j.scitotenv.2016.06.248, 2016.

Fang, Y., Chen, Y., Tian, C., Lin, T., Hu, L., Li, J., Zhang, G.: Application of PMF receptor model merging with PAHs signatures for source apportionment of black carbon in the continental shelf surface sediments of the Bohai and Yellow Seas, China, J. Geophys. Res-Oceans., 121, 1346–1359, https://doi.org/10.1002/2015JC011214, 2016.

Feng, J., Guo, Z., Chan, C.K., and Fang, M.: Properties of organic matter in $PM_{2.5}$ at Changdao Island, China - A rural site in the transport path of the Asian continental outflow, Atmos. Environ., 41, 1924–1935, https://doi.org/10.1016/j.atmosenv.2006.10.064, 2007.

Gao, Y., Guo, X., Ji, H., Li, C., Ding, H., Briki, M., Tang, L., and Zhang, Y.: Potential threat of heavy metals and PAHs in $PM_{2.5}$ in different urban functional areas of Beijing, Atmos. Res., 178-179, 6–16, https://doi.org/10.1016/j.atmosres.2016.03.015, 2016.

Gibbs, G.W.: Estimating residential polycyclic aromatic hydrocarbon (PAH) related lung cancer risks using occupational data, The Annals of Occupational Hygiene., 41, 49–53, https://doi.org/10.1093/ANNHYG/41.INHALED_PARTICLES_VIII.49, 1997.

Gong, P., Wang, X.P., and Yao, T.D.: Ambient distribution of particulate- and gas-phase n-alkanes and polycyclic aromatic hydrocarbons in the Tibetan Plateau, Environ. Earth. Sci., 64, 1703–1711, https://doi.org/10.1007/s12665-011-0974-3, 2011.

Guo, X., Zhao, L., Chen, D., Jia, Y., Zhao, N., Liu, W., and Cheng, S.: Air quality improvement and health benefit of $PM_{2.5}$ reduction from the coal cap policy in the Beijing-Tianjin-Hebei (BTH) region, China, Environ. Sci. Pollut. R., 25, 32709–32720, https://doi.org/10.1007/s11356-018-3014-y, 2018.

Han, M., Liu, S., Liu, M., Lu, M., Yan, W., He, Y., Dang, H., Dai, X., Zhang, Z., Du, X., and Meng, F.: Assessment of the effect of the reduction of the residential coal combustion on the atmospheric BaP pollution in Beijing-Tianjin-Hebei region, China Environmental Science., 38, 3262–3272, https://doi.org/10.19674/j.cnki.issn1000-6923.2018.0350-en, 2018.

Hong, W.J., Jia, H., Ma, W.L., Sinha, R.K., Moon, H.B., Nakata, H., Nguyen Hung, M., Chi, K.H., Li, W.L., Kannan, K., Sverko, E., and Li, Y.F.: Distribution, fate, inhalation exposure and lung cancer risk of atmospheric polycyclic aromatic hydrocarbons in some Asian countries, Environ. Sci. Technol., 50, 7163–7174, https://doi.org/10.1021/acs.est.6b01090, 2016.

Huang, C., Wang, Q., Wang, S., Ren, M., Ma, R., and He, Y.: Air pollution prevention and control policy in China, Adv. Exp. Med. Biol., 1017, 243–261, https://doi.org/10.1007/978-981-10-5657-4_11, 2017.

Huang, H.Y., Shi, J.F., Guo, L.W., Zhu, X.Y., Wang, L., Liao, X.Z., Liu, G.X., Bai, Y.N., Mao, A.Y., Ren, J.S., Sun, X.J., Zhang, K., He, J., Dai, M.: Expenditure and financial burden for common cancers in China: a hospital-based multicentre cross-sectional study, Lancet., 388, 10–10, https://doi.org/10.1016/S0140-6736(16)31937-7, 2016.

Jaward, T.M., Zhang, G., Nam, J.J., Sweetman, A.J., Obbard, J.P., Kobara, Y., and Jones, K.C.: Passive air sampling of polychlorinated biphenyls, organochlorine compounds, and polybrominated diphenyl ethers across Asia, Environ. Sci. Technol., 39, 8638–8645, https://doi.org/10.1021/es051382h, 2005.

~~Jia, Y.L., Stone, D., Wang, W.T., Schrlau, J., Tao, S., and Simonich, S.L.M.: Estimated reduction in cancer risk due to PAH exposures if source control measures during the 2008 Beijing Olympics were sustained, Environ. Health. Persp., 119, 815–820, https://doi.org/10.1289/ehp.1003100, 2011.~~

Li, N., Zhang, X., Shi, M., and Hewings, G.J.D.: Does China's air pollution abatement policy matter? An assessment of the Beijing-Tianjin-Hebei region based on a multi-regional CGE model, Energ. Policy., 127, 213–227, https://doi.org/10.1016/j.enpol.2018.12.019, 2019.

Li, W., Park, R., Alexandrou, N., Dryfhout-Clark, H., Brice, K., and Hung, H.: Multi-year analyses reveal different trends, sources, and implications for source-related human health risks of atmospheric polycyclic aromatic hydrocarbons in the Canadian Great Lakes Basin, Environ. Sci. Technol., 55, 2254–2264, https://doi.org/10.1021/acs.est.0c07079, 2021.

649 Li, Z.Y., Wang, Y.T., Li, Z.X., Guo, S.T., and Hu, Y.: Levels and Sources of $PM_{2.5}$-associated PAHs
650 during and after the Wheat Harvest in a Central Rural Area of the Beijing-Tianjin-Hebei (BTH)
651 Region, Aerosol. Air. Qual. Res., 20, 1070–1082, https://doi.org/10.4209/aaqr.2020.03.0083, 2020.
652 Lian, L., Huang, T., Ling, Z., Li, S., Li, J., Jiang, W., Gao, H., Tao, S., Liu, J., Xie, Z., Mao, X.,
653 Ma, J.: Interprovincial trade driven relocation of polycyclic aromatic hydrocarbons and lung cancer
654 risk in China, J. Clean. Prod., 280, 124368, https://doi.org/10.1016/j.jclepro.2020.124368, 2021.
655 Liang, X., Tian, C., Zong, Z., Wang, X., Jiang, W., Chen, Y., Ma, J., Luo, Y., Li, J., Zhang, G.: Flux
656 and source-sink relationship of heavy metals and arsenic in the Bohai Sea, China, Environ. Pollut.,
657 242, 1353-1361, https://doi.org/10.1016/j.envpol.2018.08.011, 2018.
658 Lin, Y., Ma, Y., Qiu, X., Li, R., Fang, Y., Wang, J., Zhu, Y., and Hu, D.: Sources, transformation,
659 and health implications of PAHs and their nitrated, hydroxylated, and oxygenated derivatives in
660 $PM_{2.5}$ in Beijing, Journal of Geophysical Research., 120, 7219–7228,
661 https://doi.org/10.1002/2015JD023628, 2015.
662 Liu, H., Li, B., Qi, H., Ma, L., Xu, J., Wang, M., Ma, W., and Tian, C.: Source apportionment and
663 toxic potency of polycyclic aromatic hydrocarbons (PAHs) in the air of Harbin, a cold city in North-
664 ern China, Atmosphere-Basel., 12, https://doi.org/10.3390/atmos12030297, 2021.
665 ~~Liu, L., Zhen, X., Wang, X., Li, Y., Sun, X., and Tang, J.: Legacy and novel halogenated flame~~
666 ~~retardants in seawater and atmosphere of the BS: Spatial trends, seasonal variations, and influenc-~~
667 ~~ing factors, Water. Res., 184, https://doi.org/10.1016/j.watres.2020.116117, 2020.~~
668 Liu, W.J., Xu, Y.S., Zhao, Y.Z., Liu, Q.Y., Yu, S.Y., Liu, Y., Wang, X., Liu, Y., Tao, S., and Liu,
669 W.X.: Occurrence, source, and risk assessment of atmospheric parent polycyclic aromatic hydro-
670 carbons in the coastal cities of the Bohai and Yellow Seas, China, Environ. Pollut., 254,
671 https://doi.org/10.1016/j.envpol.2019.113046, 2019.
672 Luo, M., Ji, Y.Y., Ren, Y.Q., Gao, F.H., Zhang, H., Zhang, L.H., Yu, Y.Q., and Li, H.: Characteristics
673 and health risk assessment of $PM_{2.5}$-bound PAHs during heavy air pollution episodes in winter in
674 urban area of Beijing, China, Atmosphere-Basel., 12, 323, https://doi.org/10.3390/atmos12030323,
675 2021.

设置了格式: 下划线

带格式的: 正文, 行距: 单倍行距

设置了格式: 字体: (默认) Times New Roman, 小四, 下划线

设置了格式: 字体颜色: 自定义颜色(RGB(59,54,250))

Lv, Min., Luan, Xiaolin., Liao, Chunyang., Wang, Dongqi., Liu, Dongyan., Zhang, Gan., Jiang, Guibin., Chen, Lingxin.: Human impacts on polycyclic aromatic hydrocarbon distribution in Chinese intertidal zones, Nature Sustainability., https://doi.org/10.1038/s41893-020-0565-y, 2020.

Ma, W.L., Li, Y.F., Qi, H., Sun, D.Z., Liu, L.Y., and Wang, D.G.: Seasonal variations of sources of polycyclic aromatic hydrocarbons (PAHs) to a northeastern urban city, China, Chemosphere., 79, 441–447, https://doi.org/10.1016/j.chemosphere.2010.01.048, 2010.

Ma, W.L., Liu, L.Y., Jia, H.L., Yang, M., and Li, Y.F.: PAHs in Chinese atmosphere Part I: Concentration, source and temperature dependence, Atmos. Environ., 173, 330–337, https://doi.org/10.1016/j.atmosenv.2017.11.029, 2018.

Ma, W.L., Zhu, F.J., Liu, L.Y., Jia, H.L., Yang, M., and Li, Y.F.: PAHs in Chinese atmosphere Part II: Health risk assessment, Ecotox. Environ. Safe., 200, 110774, https://doi.org/10.1016/j.ecoenv.2020.110774, 2020.

Ma, Y.X., Xie, Z.Y., Yang, H.Z., Moller, A., Halsall, C., Cai, M.H., Sturm, R., and Ebinghaus, R.: Deposition of polycyclic aromatic hydrocarbons in the North Pacific and the Arctic, J. Geophys. Res-Atmos., 118, 5822–5829, https://doi.org/10.1002/jgrd.50473, 2013.

Marvin, C.H., Tomy, G.T., Thomas, P.J., Holloway, A.C., Sandau, C.D., Idowu, I., and Xia, Z.: Considerations for prioritization of polycyclic aromatic compounds as environmental contaminants, Environ. Sci. Technol., 54, 14787–14789, https://doi.org/10.1021/acs.est.0c04892, 2020.

Menzler, S., Piller, G., Gruson, M., Rosario, A.S., Wichrnann, H.E., and Kreienbrock, L.: Population attributable fraction for lung cancer due to residential radon in Switzerland and Germany, Health. Phys., 95, 179–189, https://doi.org/10.1097/01.Hp.0000309769.55126.03, 2008.

Moeckel, C., Harner, T., Nizzetto, L., Strandberg, B., Lindroth, A., and Jones, K.C.: Use of depuration compounds in passive air samplers: results from active sampling-supported field deployment, potential uses, and recommendations, Environ. Sci. Technol., 43, 3227–3232, https://doi.org/10.1021/es802897x, 2009.

Paatero, P., Eberly, S., Brown, S.G., and Norris, G.A.: Methods for estimating uncertainty in factor analytic solutions, Atmos. Meas. Tech., 7, 781–797, https://doi.org/10.5194/amt-7-781-2014, 2014.

设置了格式: 下划线

~~Qin, F., Liu, H.Y., Jing, L., Liu, W., Yin, J., and Wei, X.D.: The investigation of energy consumption in the village of Jilin province, Journal of Jilin Jianzhu University (China)., 2, 37–40, https://d.wanfangdata.com.cn/periodical/jljzgcxyxb200702011, 2007.~~

Qu, L., Yang, L., Zhang, Y., Wang, X., Sun, R., Li, B., Lv, X., Chen, Y., Wang, Q., Tian, C., and Ji, L.: Source Apportionment and Toxic Potency of $PM_{2.5}$-Bound Polycyclic Aromatic Hydrocarbons (PAHs) at an Island in the Middle of Bohai Sea, China, Atmosphere., 13, https://doi.org/10.3390/atmos13050699, 2022.

Shi, C.L., Lou, P.A., Shi, J.F., Huang, H.Y., Li, J., Yue, Y.P., Wang, L., Dong, Z.M., Chen, P.P., Zhang, P., Zhao, C.Y., Li, F., Zhou, J.Y., and Dai, M.: Economic burden of lung cancer in mainland China,1996-2014: a systematic review, China Journal of Public Health., 33, 1767–1774, https://doi.org/10.11847/zgggws2017-33-12-25, 2017.

Sofowote, U.M., Hung, H., Rastogi, A.K., Westgate, J.N., Deluca, P.F., Su, Y.S., and McCarry, B.E.: Assessing the long-range transport of PAH to a sub-Arctic site using positive matrix factorization and potential source contribution function, Atmos. Environ., 45, 967–976, https://doi.org/10.1016/j.atmosenv.2010.11.005, 2011.

Sun, R., Wang, X., Tian, C., Zong, Z., Ma, W., Zhao, S., Wang, Y., Tang, J., Cui, S., Li, J., and Zhang, G.: Exploring source footprint of Organophosphate esters in the Bohai Sea, China: Insight from temporal and spatial variabilities in the atmosphere from June 2014 to May 2019, Environ. Int., 159, https://doi.org/10.1016/j.envint.2021.107044, 2022.

Sun, Z., Zong, Z., Tian, C., Li, J., Sun, R., Ma, W., Li, T., Zhang, G.: Reapportioning the sources of secondary components of PM2.5: combined application of positive matrix factorization and isotopic evidence. Science of the Total Environment, 764, https://doi.org/10.1016/j.scitotenv.2020.142925, 2021.

Tan, J.H., Bi, X.H., Duan, J.C., Rahn, Kenneth A., Sheng, G.Y., and Fu, J.M.: Seasonal variation of particulate polycyclic aromatic hydrocarbons associated with PM_{10} in Guangzhou, China, Atmos. Res., 80, 250–262, https://doi.org/10.1016/j.atmosres.2005.09.004, 2006.

Tian, C., Ma, J., Liu, L., Jia, H., Xu, D., and Li, Y.F.: A modeling assessment of association between

设置了格式: 下划线

East Asian summer monsoon and fate/outflow of α-HCH in Northeast Asia, Atmos. Environ., 43, 3891-3901, https://doi.org/https://doi.org/10.1016/j.atmosenv.2009.04.056, 2009.

Tong, L., Peng, C.H., Huang, Z.W., Zhang, J.J., Dai, X.R., Xiao, H., Xu, N.B., and He, J.: Identifying the pollution characteristics of atmospheric polycyclic aromatic hydrocarbons associated with functional districts in Ningbo, China, B. Environ. Contam. Tox., 103, 34–40, https://doi.org/10.1007/s00128-018-02535-4, 2019.

Wang, X.P., Zong, Z., Tian, C.G., Chen, Y.J., Luo, C.L., Tang, J.H., Li, J., Zhang, G.: Assessing on toxic potency of $PM_{2.5}$-bound polycyclic aromatic hydrocarbons at a national atmospheric background site in North China, Sci. Total. Environ., 612, 330–338, https://doi.org/10.1016/j.scitotenv.2017.08.208, 2018.

Wu, D., Xu, Y., and Zhang, S.: Will joint regional air pollution control be more cost-effective? An empirical study of China's Beijing-Tianjin-Hebei region, J. Environ. Manage., 149, 27–36, https://doi.org/10.1016/j.jenvman.2014.09.032, 2015.

Xing, X., Chen, Z., Tian, Q., Mao, Y., Liu, W., Shi, M., Cheng, C., Hu, T., Zhu, G., Li, Y., Zheng, H., Zhang, J., Kong, S., and Qi, S.: Characterization and source identification of $PM_{2.5}$-bound polycyclic aromatic hydrocarbons in urban, suburban, and rural ambient air, central China during summer harvest, Ecotox. Environ Safe., 191, https://doi.org/10.1016/j.ecoenv.2020.110219, 2020.

Yan, Z., Jin, L., Chen, X., Wang, H., Tang, Q., Wang, L., and Lei, Y.: Assessment of air pollutants emission reduction potential and health benefits for residential heating coal changing to electricity in the Beijing-Tianjin-Hebei region, Research of Environmental Sciences., 32, 95–103, https://doi.org/10.13198/j.issn.1001-6929.2018.10.16, 2019.

Yang, Q.Q., Yuan, Q.Q., Li, T.W., Shen, H.F., and Zhang, L.P.: The relationships between $PM_{2.5}$ and meteorological factors in China: seasonal and regional variations, Int. J. Env. Res. Pub. He., 14, https://doi.org/10.3390/ijerph14121510, 2017.

754 Yu, Q.Q., Gao, B., Li, G.H., Zhang, Y.L., He, Q.F., Deng, W., Huang, Z.H., Ding, X., Hu, Q.H.,
755 Huang, Z.Z., Wang, Y.J., Bi, X.H., and Wang, X.M.: Attributing risk burden of $PM_{2.5}$-bound poly-
756 cyclic aromatic hydrocarbons to major emission sources: Case study in Guangzhou, south China,
757 Atmos. Environ., 142, 313–323, https://doi.org/10.1016/j.atmosenv.2016.08.009, 2016.
758 Zhang, J., Liu, W., Xu, Y., Cai, C., Liu, Y., Tao, S., and Liu, W.: Distribution characteristics of and
759 personal exposure with polycyclic aromatic hydrocarbons and particulate matter in indoor and out-
760 door air of rural households in Northern China, Environ. Pollut., 255, 113176,
761 https://doi.org/10.1016/j.envpol.2019.113176, 2019.
762 Zhang, J.W., Feng, L.H., Zhao, Y., Hou, C.C., and Gu, Q.: Health risks of $PM_{2.5}$-bound polycyclic
763 aromatic hydrocarbon (PAH) and heavy metals (PPAH&HM) during the replacement of central
764 heating with urban natural gas in Tianjin, China, Environ. Geochem. Hlth., 44, 2495–2514,
765 https://doi.org/10.1007/s10653-021-01040-8, 2021.
766 Zhang, J.W., Zhao, J., Cai, J., Gao, S.T., Li, J., Zeng, X.Y., and Yu, Z.Q.: Spatial distribution and
767 source apportionment of atmospheric polycyclic aromatic hydrocarbons in the Pearl River Delta,
768 China, Atmos. Pollut. Res., 9, 887–893, https://doi.org/10.1016/j.apr.2018.02.004, 2018.
769 Zhang, S.W., Chen, W.Q., Kong, L.Z., Li, G.L., and Zhao, P.: An Annual Report: Cancer Incidence
770 in 35 Cancer Registries in China, 2003, China Cancer., 494–507,
771 https://doi.org/10.3969/j.issn.1004-0242.2007.07.001, 2007.
772 Zhang, Y.J., Lin, Y., Cai, J., Liu, Y., Hong, L.N., Qin, M.M., Zhao, Y.F., Ma, J., Wang, X.S., Zhu,
773 T., Qiu, X.H., and Zheng, M.: Atmospheric PAHs in North China: Spatial distribution and sources,
774 Sci. Total. Environ., 565, 994–1000, https://doi.org/10.1016/j.scitotenv.2016.05.104, 2016.
775 Zhang, Y.X., Tao, S., Cao, J., and Coveney, R.M.: Emission of polycyclic aromatic hydrocarbons
776 in China by county, Environ. Sci. Technol., 41, 683–687, https://doi.org/10.1021/es061545h, 2007.
777 Zhang, Y.X., Tao, S., Shen, H.Z., and Ma, J.M.: Inhalation exposure to ambient polycyclic aromatic
778 hydrocarbons and lung cancer risk of Chinese population, P. Natl. Acad. Sci. USA., 106,
779 21063–21067, https://doi.org/10.1073/pnas.0905756106, 2009.
780 Zhao, H., Wu, R., Liu, Y., Cheng, J., Geng, G., Zheng, Y., Tian, H., He, K., and Zhang, Q.: Air

pollution health burden embodied in China's supply chains, Environmental Science and Ecotechnology., 16, 100264–100264, https://doi.org/10.1016/j.ese.2023.100264, 2023.

Zhi, Z., Wang, W., Cheng, M., Liu, S., Xu, J., He, Y., and Meng, F.: The contribution of residential coal combustion to $PM_{2.5}$ pollution over China's Beijing-Tianjin-Hebei region in winter, Atmos. Environ., 159, 147–161, https://doi.org/10.1016/j.atmosenv.2017.03.054, 2017.

Zhu, D., Tao, S., Wang, R., Shen, H., Huang, Y., Shen, G., Wang, B., Li, W., Zhang, Y., Chen, H., Chen, Y., Liu, J., Li, B., Wang, X., Liu, W.: Temporal and spatial trends of residential energy consumption and air pollutant emissions in China. Applied Energy 106, 17-24, https://doi.org/10.1016/j.apenergy.2013.01.040, 2013.

Zhuo, S., Shen, G., Zhu, Y., Du, W., Pan, X., Li, T., Han, Y., Li, B., Liu, J., Cheng, H., Xing, B., and Tao, S.: Source-oriented risk assessment of inhalation exposure to ambient polycyclic aromatic hydrocarbons and contributions of non-priority isomers in urban Nanjing, a megacity located in Yangtze River Delta, China, Environ. Pollut., 224, 796–809, https://doi.org/10.1016/j.envpol.2017.01.039, 2017.

设置了格式: 下划线